4. Synthesis of polystyrenes with higher generation dendritic wedges by the macromonomer routes

4.1. General comments

Synthesis of higher generation (above 2) dendronized polymers with high molar mass is a challenge to chemists. As pointed out above, principally, two different synthetic routes to such polymers (Scheme 1) are available. The intrinsic problems of both routes become the more serious and limiting, the more sterically demanding the dendrons are. The problems associated with route A have something to do with steric hindrance. Here the critical point is the steric demand of both monomer and chain end. Incoming monomer will only be connected to the chain end if the steric hindrance is not too high. Otherwise this process will be slowed or even rendered impossible.

An obviously critical issue associated with route B is achieving a complete coverage of the backbone anchor groups with dendrons. If large dendrons are to be attached, steric hindrance also comes into play for two reasons: a) the shielding of still available anchor groups on the backbone by dendrons already attached in close proximity and b) the conformation of the dendron, which may lead to a self-shielding of the functional group at the focal point through which the attachment ought to take place.

Although there are drawbacks to both routes, progress has been made for both in our group. From monomer route, by polycondensation, poly(*para*-phenylene) with G4 Frechet-type dendrons has been obtained for the first time with P_n = 25 and P_w= 125 (according to GPC) on a gram scale. The attach-to route met here only with limited success. Complete coverage has not been achieved yet beyond second generation (G2). This route has its advantage, however, especially as far as high molar mass dendronized polymers with low generation dendrons are concerned.

From the previous experiments of using the attach-to route, the structure characterisation of the resulting polymers became the more difficult the highe the generation of attached dendrons. In order to further explore the potential of the attach-to route, it was necessary to prepare some reference (or model) polymers with the same structures obtained by the attach-to route.

4.2. Synthesis of G2 and G3 polymers with protected amino functional groups by macromonomer route

The creation of a peptide linkage between two amino acid segments is one of the most important reactions in organic and bioorganic chemistry.[34,35] In the above chapter, synthesis of unpolar dendrons with amino functional groups were described. Dendrons with carboxyl acid functional groups have also been prepared previously in our group. By using peptide chemistry, larger dendrons would be accessible by amide bond formation between the carboxylic acid function of one dendron and the amino group of another dendron. Higher generation dendronized polymers may be synthesised by converting these larger dendrons into monomers followed by their radical polymerisation.

Carbodiimides have a cumulative double-bond system which reacts with many types of functional groups. They have been particularly valuable in the synthesis of peptides and

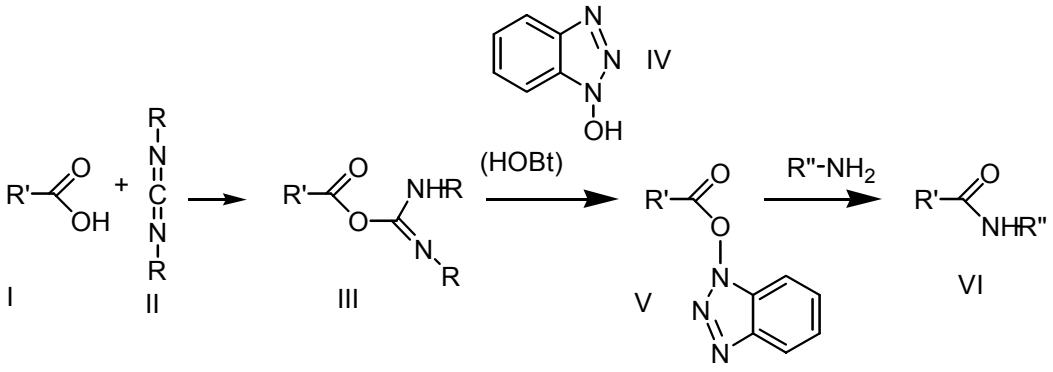

Scheme 12. Principal of the formation of amide by HOBt/EDC method.

of nucleotides because of their water withdrawing capability in acylations under mild conditions. Amide formation of terminal amines with focal carboxylic acids in the presence of carbodiimides and HOBt has been used in the synthesis of dendrons. The basic principle are shown in Scheme 12. It involves the reaction of carbonic acid (I) and

carbodiimide (II) with the formations of (III). Treatment of (III) with HOBt (IV) will yield an activated ester (V) which reacts with the amine to give amide (VI).

4.2.1. Synthesis of G2, G3 and G4 dendrons

The synthesis of G2 dendron (**18**) was carried out by the EDC/HOBt method. For the preparations of G3 and G4 dendrons, The same method was also employed, but it turned out that the purification of the resulting dendrons was difficult. To facilitate the purification, activated Esters were used directly. The corresponding activated Esters **19b** and **21b** were prepared by treatment of **19a** and **21a** in dichloride methylene with N-hydroxysuccinimide and N, N'-Dicyclohexyl Carbodiimide (DCC) for 24 h at room temperature. The resulting precipitate was filtered. Chromatographic separation gave **19b** and **21b** in 89% and 45% yield. As can be seen, the yield for this activation step decrease with the increase of generation. The structures of the resulted activated dendrons were confirmed by common methods.

Reactions of **13c** with activated Esters **19b** and **21b** in the presence of triethylamine gave corresponding G3 (**20**)and G4 dendrons **22** in 89% and 57% yields, respectively.

The structures of the dendrons were confirmed by ^{1}H and ^{13}C NMR spectroscopy, mass spectrometry and correct data from element analysis. Figure 7a and 7b show the ^{1}H

and ^{13}C NMR spectra of **20**. Normally, allylic functional group shows three typical absorptions in proton NMR spectrum at 3.2, 5.0 and 5.9 ppm. Because protons 3 and 26 overlap at 3.2 ppm, the dublet peak of 3 should not be observed here. Teoc functional groups have the typical absorptions at –0.05, 0.90 and 4.10 ppm. The protected amine groups appear in the range of δ = 4.8-5.2 as two broad peaks centred at 4.83 (minor) (there is overlap with H1) and 5.12 (major). The inner protons of the amide group appear at 7.18. ^{1}H NMR of compound **22** is shown in Figure 9. All the signals are in full agreement with the structure described. The amine protected protons appear at the range of 4.70 to 5.14 ppm. The other two sets of amide protons occur at 7.25 (H27) and 7.05 (H17). All the other peaks were assigned, and the integrations are in agreement with the

number. The absorption in the ^{13}C NMR spectrum also appear as anticipated. The protecting group Teoc appears at δ = -1.5, 17.5, 62.6 and 156.8. The allylic functional

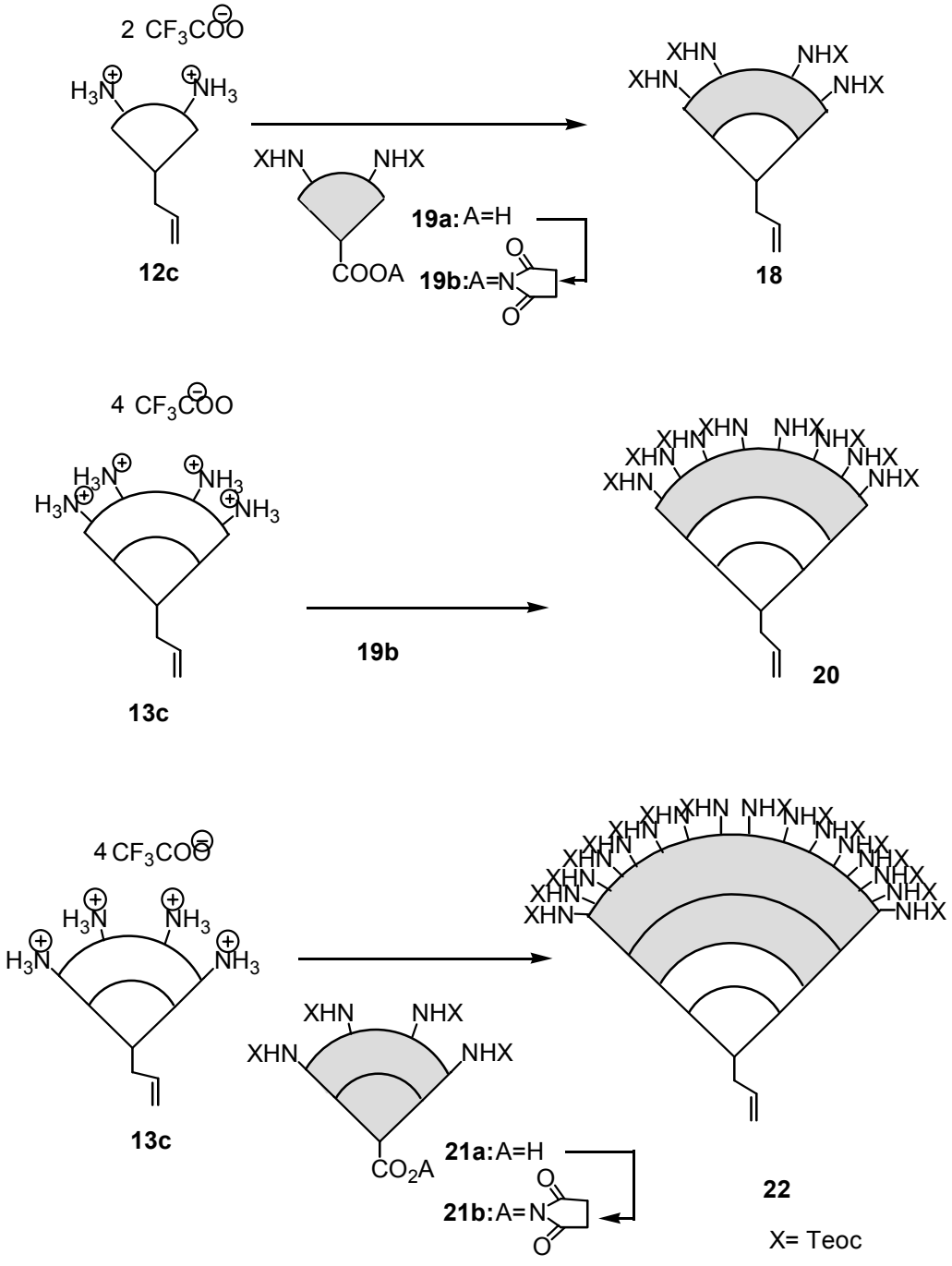

Scheme 13. Synthesis of G2 (**18**), G3 (**20**) and G4 (**22**) dendrons.

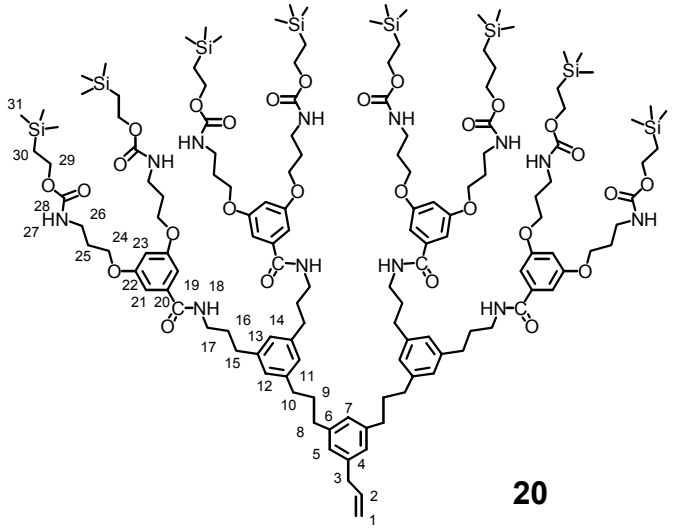

20

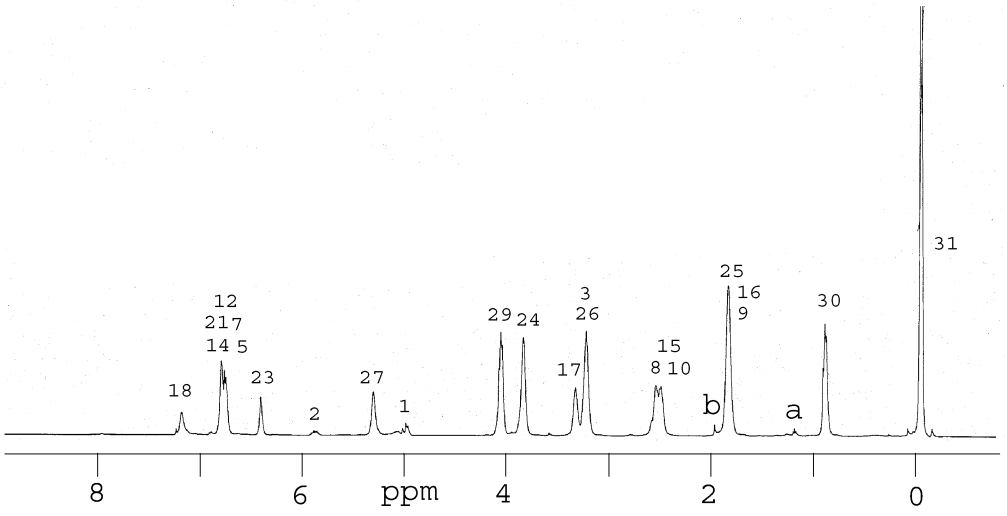

Fig. 7a. ^{1}H NMR spectum (500 MHz) of G3 dendron **13** with signal assignment.
(Peaks a and b from residual solvent)

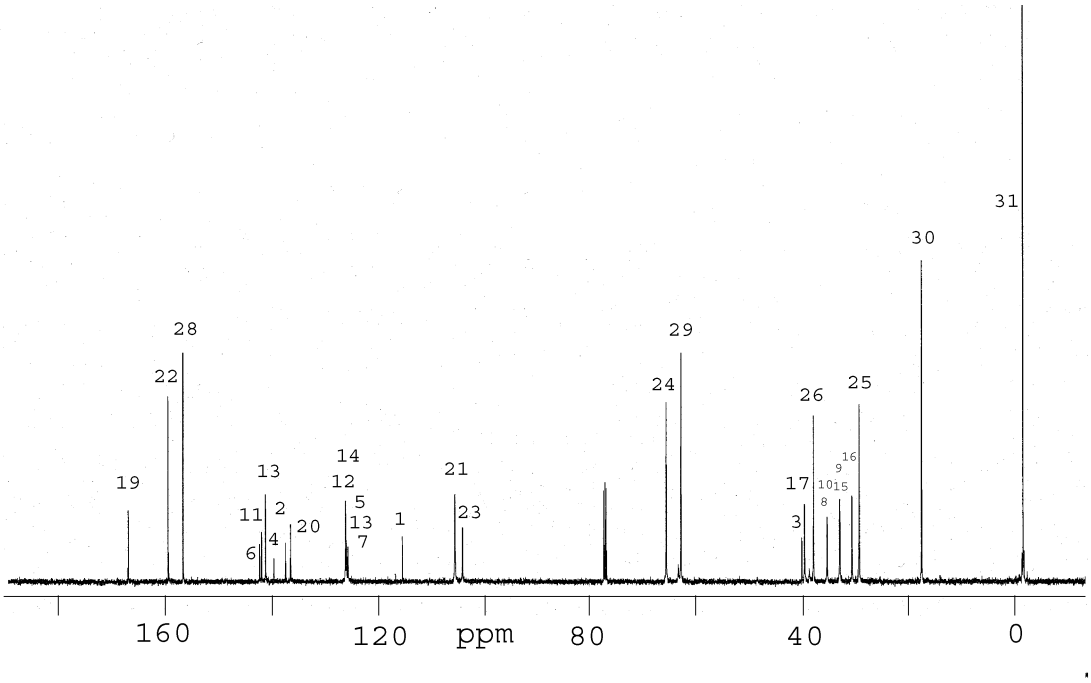

Fig. 7b. ^{13}C NMR (125 MHz) spectrum of G3 dendron **20** with signal assignment.

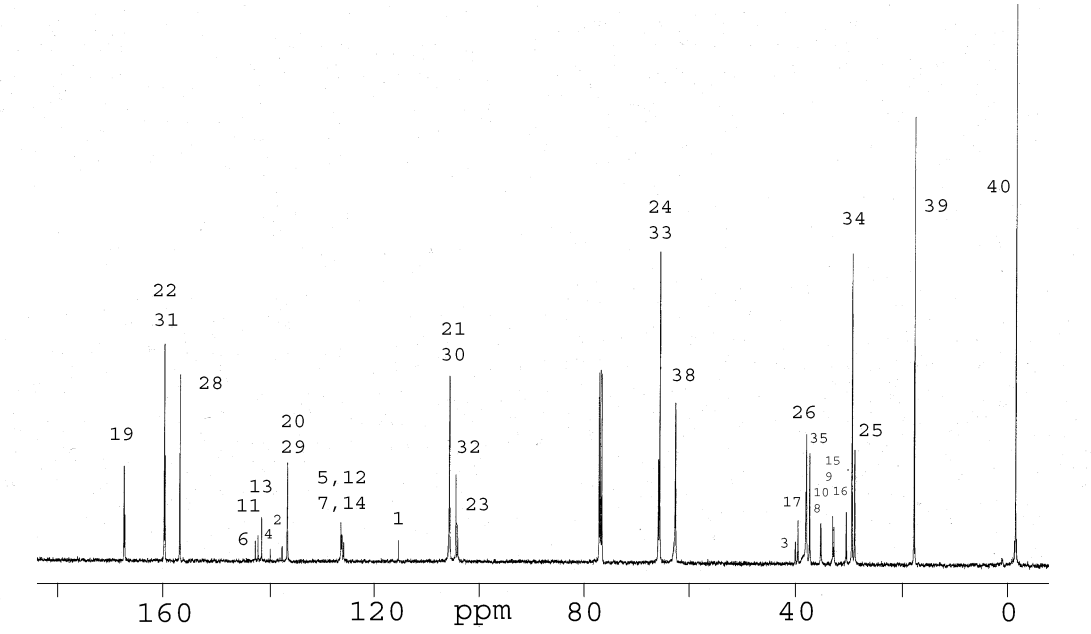

Fig. 8. ^{13}C NMR spectrum of G4 dendron **22** in $CDCl_3$ with signal assignment. (PG stands for Teoc protecting group) (The chemical structure is presented in Figure 9)

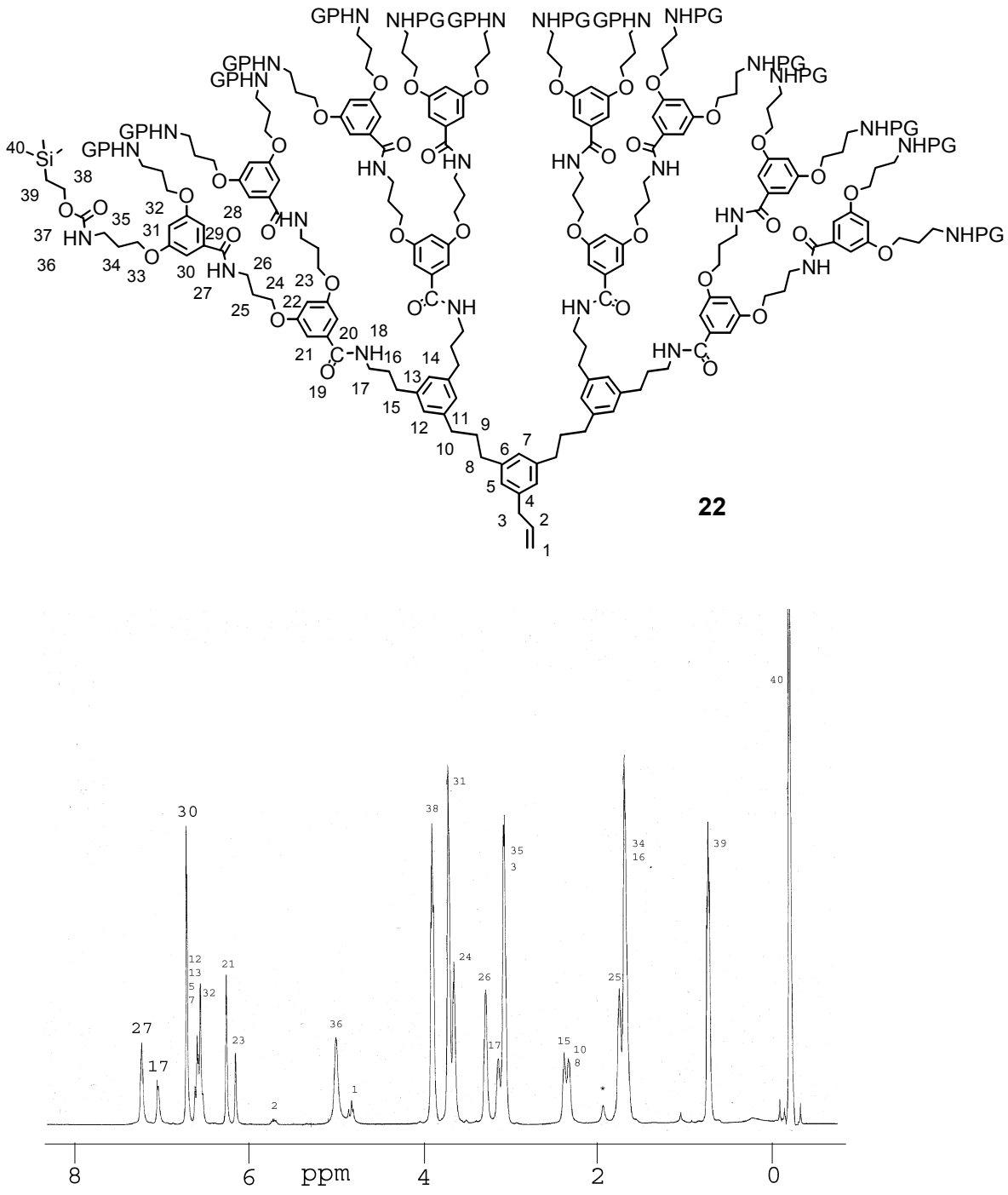

Fig. 9. ^{1}H NMR spectrum of G4 dendron **22** in $CDCl_3$ with signal assignment.

group appears at δ = 115.3, 137.4 and 39.9 ppm. Compound **22** has a similar structure as **20.** Its ^{13}C NMR spectrum is shown in Figure 8**.** The resonances of C20 and C28 appear at 167.2 and 167.4, whereas those of C22 and C31 occur at 159.7 and 159.8, and those of C24 and C33 at 66.0 and 65.8. The resonances of these three sets of carbon atoms appear almost at the same shift in the NMR spectrum because of their similar chemical surroundings. All the other peaks appear as expected.

4.2.2. Synthesis of G2 and G3 macromonomers

The synthesis of G2 and G3 macromonomers was performed according to the same procedure as described above. Scheme 12 depicts the synthetic sequences to monomers **23** and **24**. Cross-coupling of 4-bromo styrene with the adduct of **18** or **20** with 9-BBN yielded monomers **23** and **24** in 56% and 40%, respectively. It is found that the conversion of hydroboration of allylic dendrons decreases with the increase of dendrons' generation. For G4 dendron **22**, this step becomes more serious. The yield for the hydroboration step is near 60% (according to NMR). Attempts to separate the unreacted raw material were not successful. In spite of the presence of **22**, the next cross-coupling reaction was tried according to the same procedures as for **23** or **24**. Unfortunately, although column chromatograph separations have been tried for 3 times. the G4 monomer was not available, This also demonstrates the difficulty for the synthesis of higher generation monomers.

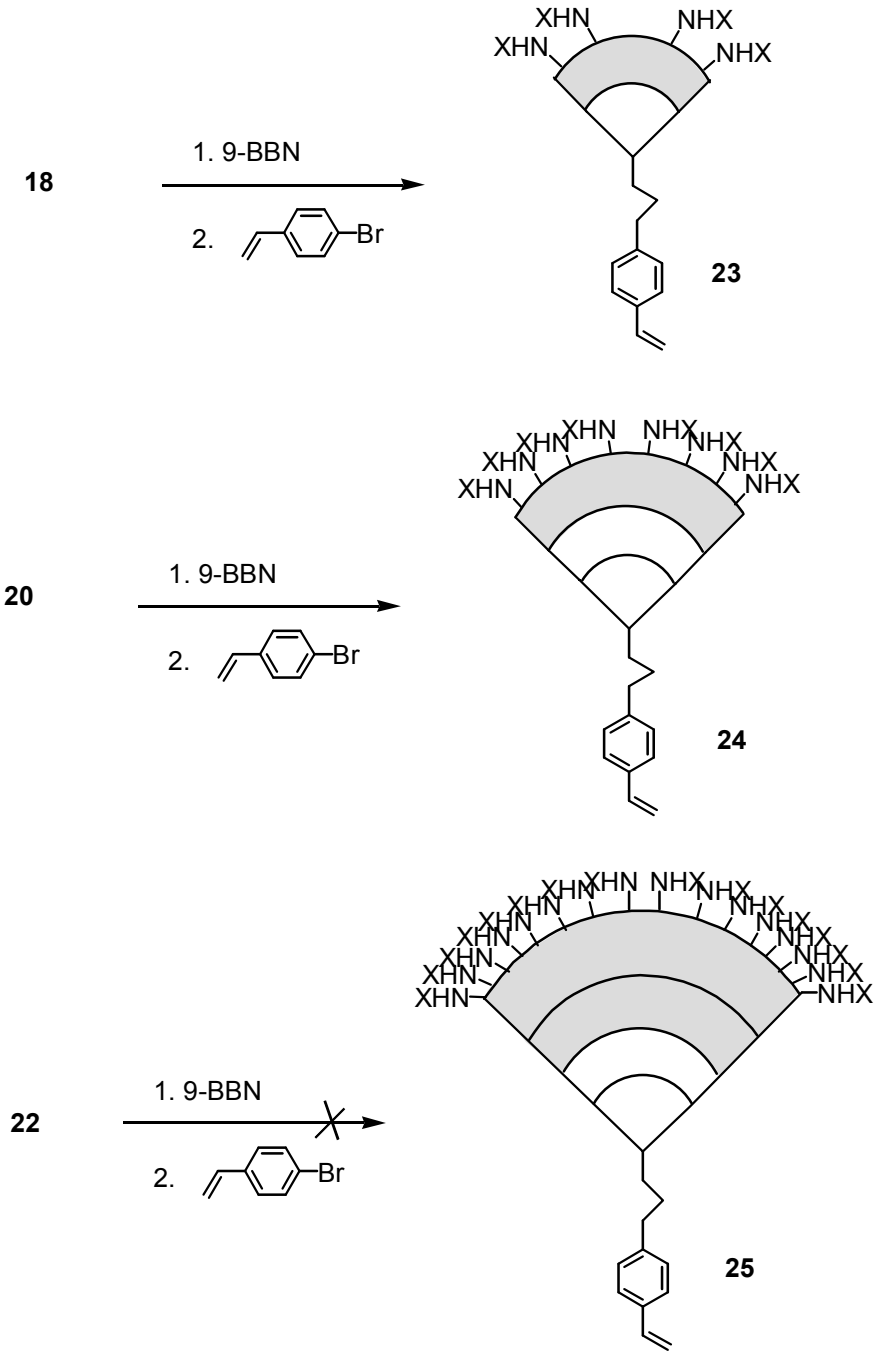

Scheme 12. Synthesis of G2 (**23**) and G3 (**24**) monomers. For the synthesis of **25**, see text.

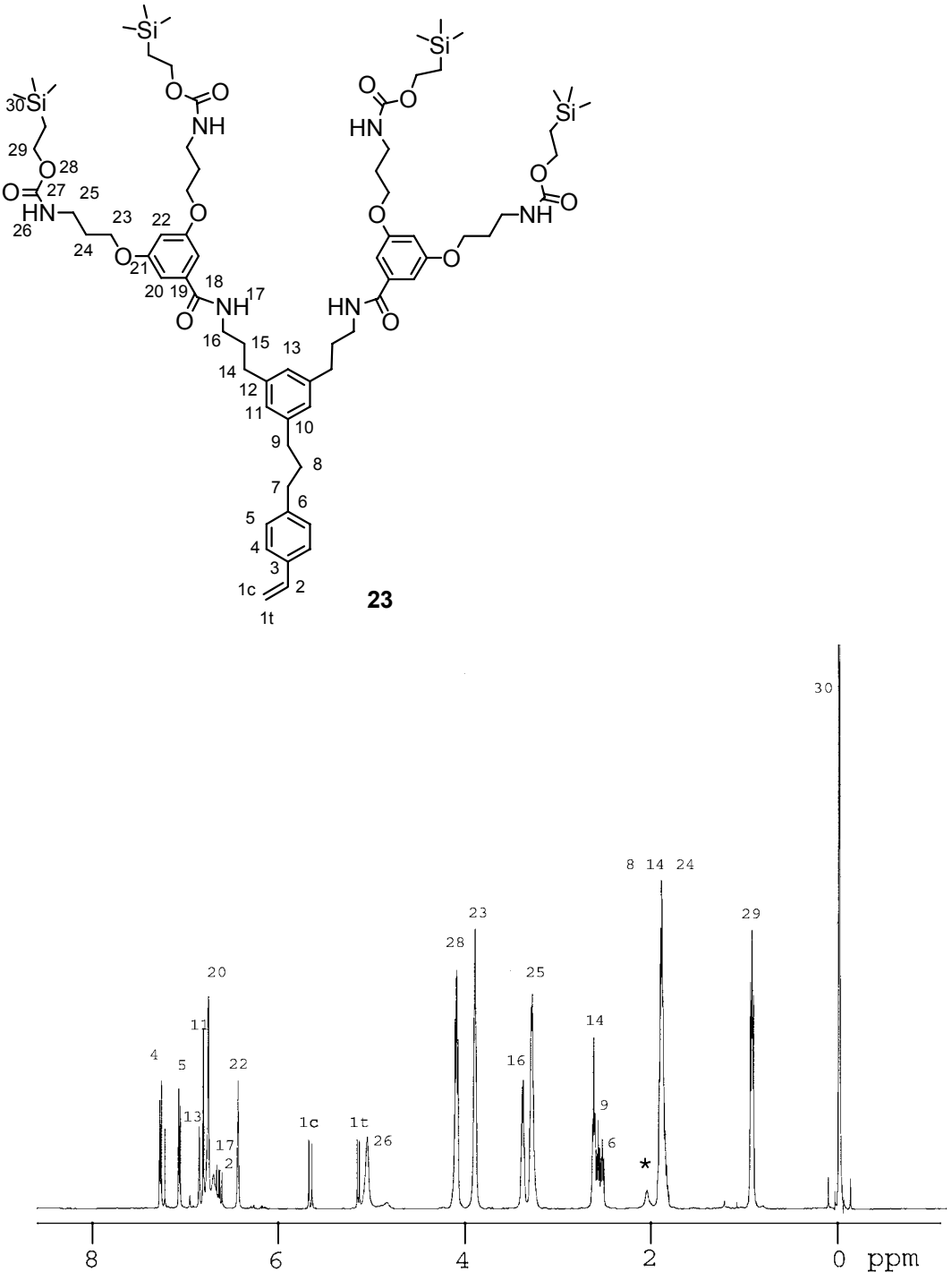

Fig. 10a. ^{1}H NMR (500 MHz) spectra of G2 monomer **23**.

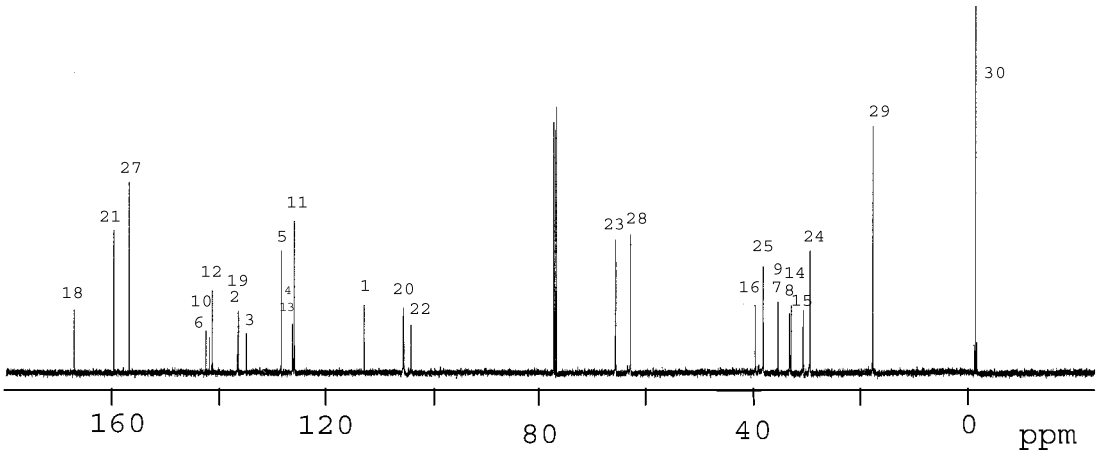

Fig. 10b. ^{13}C NMR (125 MHz) spectrum of G2 monomer **23**. (the structure is given in Figure 10a)

The ^{1}H NMR spectrum of monomer **23** is presented in Figure 10a. The vinyl group appears at δ = 5.2, 5.7 and 6.6 ppm. The protons of the protected amine groups in $CDCl_3$ absorb in the range of δ = 4.8-5.2 as two broad peaks centred at 4,83 (minor) and 5.12 (major). The integration of the whole range corresponds to 4H (assigned to the protons of amides at the outer layer. The protons of amide at the inner layer absorb at 6.6 ppm, which overlaps with the aromatic ones. It is interesting that H7, H9 and H14, which connect benzene and methylene groups, appear separately in the 500 MHz ^{1}H NMR spectrum, whereas in 270 Hz NMR spectrometer, it shows only one peak. ^{13}C NMR spectrum (Figure 10b) has also been recorded. All the resonances can be assigned and are in full agreement with the structure described.

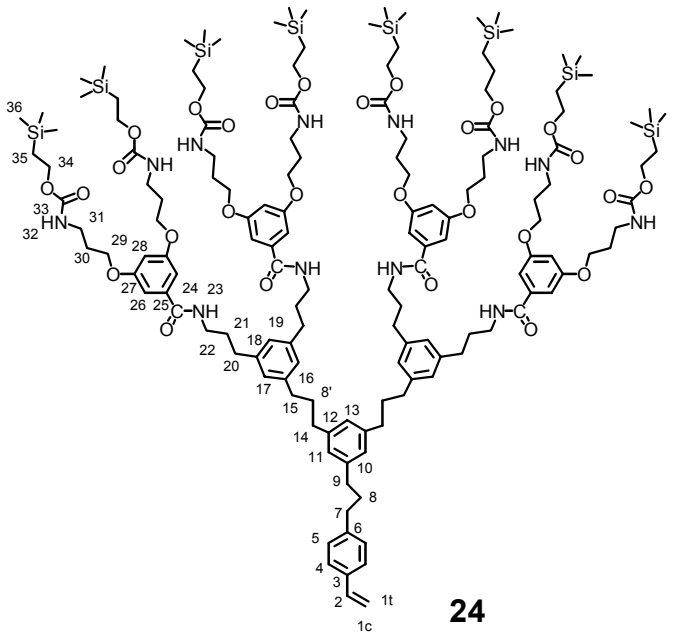

24

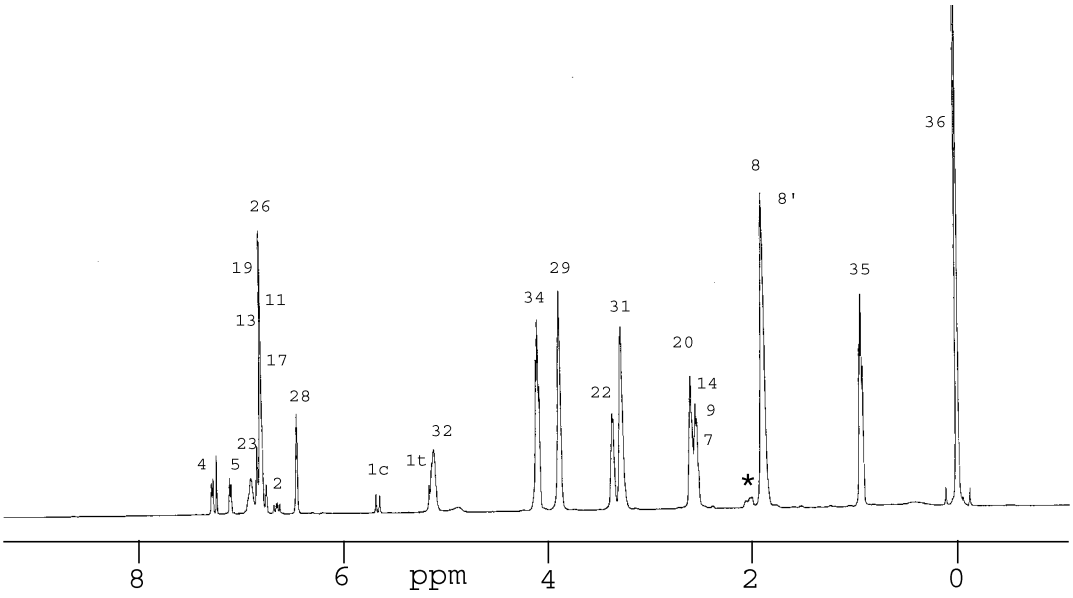

Fig. 11a. ^{1}H NMR (125 MHz) spectrum of G3 monomer **24** in $CDCl_3$ with signal assignment.

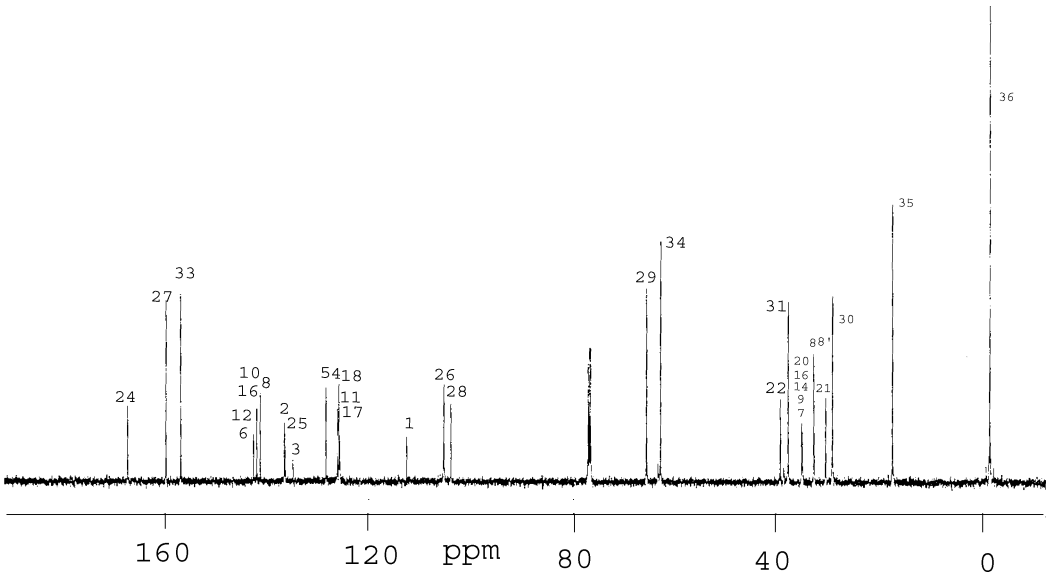

Fig. 11b. ^{13}C NMR (125 MHz) spectrum of G3 monomer **24** in $CDCl_3$ with signal assignment. (For structure see Figure 11a)

Figure 11a records the ^{1}H (500 MHz) for G3 monomer **24** in $CDCl_3$. As can be seen, the spectrum is in full agreement with the proposed structure. The protons of the protected amine groups in $CDCl_3$ absorb in the range of δ = 4.8-5.2 as two broad peaks centred at 4,83 (minor) and 5.12 (major). The integration of the whole range corresponds to 8H (assigned to the protons of amides at the outer layer). The protons of amide at the inner layer absorb at 6.6 ppm after subtracting the integration of one proton arising from the vinyl group. The absorption of the protons in the inner layer appears at 6.90. The proton spectra normally show a signal at 2.05 ppm in varying intensities which is tentatively assigned to water. The ^{13}C NMR (125 MHz) is exhibited in Figure 11b with full assignment.

Attempts to prepare G4 monomer (styrenic type) were not successful. The main problems accounted for here was that the conversion rate was low (around 50-60%) for the hydroboration of G4 dendron. Consequently, it rendered the purification of G4 monomer impossible. Increasing the temperature of hydroboration to 60°C or the ratio

of molarity of 9-BBN to **22** did not improve the conversation rate significantly. This case also illustrates the difficulty of obtaining higher generation monomers.

4.2.3. Polymerisation of G2 and G3 monomers 23 and 24

Radical polymerisation of monomer **23** and **24** were carried out at 90 °C with BPB as initiators. The crude polymers were dissolved in THF, precipitated with methanol/water (4:1/V:V), and lyophilised from benzene. Molecular weights were determined by GPC with tetrahydrofuran as the eluent and polystyrene as standards.

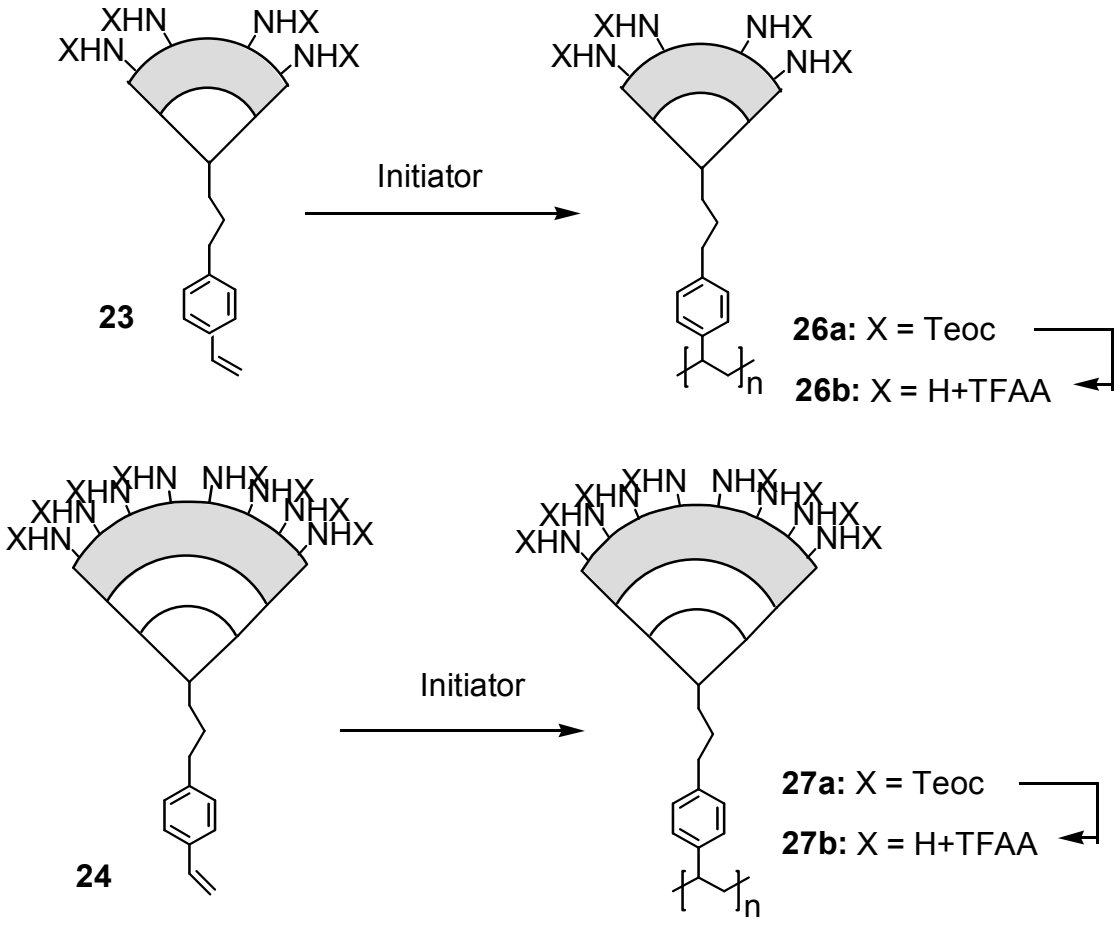

Scheme 15. Polymerisations of monomers **23** and **24**.

For the polymerization of dendronized monomers, the concentration of the reaction medium plays an absolutely important role in the polymerization of macromonomers. this may go so far that below a certain concentration polymerization is not only slowed down but rather rendered impossible.

For this G2 monomer **23**, the dependence of molar mass on concentration was investigated systematically for c_m = 34-64 %, where c_m is the concentration of monomer in weight percent. As can be seen from Figure 12, there is only a narrow concentration window in which polymerisation proceeds satisfactorily. Below c_m = 45% the monomer practically does not polymerize at all; molar mass are in the oligomer regime and yields are poor. Molar masses and yields increase sharply between c_m = 45 and 53 %, whereby the masses pass through a maximum. For concentrations higher than c_m = 53%, yields remain more or less constant; molar masses, however, decrease quickly until a plateau is reached. Similar results were observed by Tsukahara et al.[36] for macromonomers with oligostyrene side chains. Additionally they observed threshold molarities (M), at which the steep increase occurs rapidly, and shifts to higher values as the molecular weight of the macromonomer decrease. For monomers with roughly 12500 and 4.500 $gmol^{-1}$, they observed threshold molarities of [M] = 0.04 and 0.1 M, respectively.

Unfortunately the molarity of the solutions of monomer **23** could not be determined with sufficient accuracy for concentrations higher than 59 wt.-%, rendering a sound comparison of the above experiments with those reported by Tsukahara et al. impossible. Qualitatively, however, monomer **23** lies in the trend. A possible explanation for the observed maximum may be that after a few growth steps the oligomer adopts a spherical shape with the radical chain end somewhat in its interior. At low morality, this results in a sharp concentration gradient from the interior of the sphere to the surrounding solution against which the monomer has to diffuse to reach the chain end. In other words, the concentration gradient protects the radical chain end. As monomer concentration in solution and in the spheres (here: monomer = pendant dendrons) becomes similar, there is no gradient anymore and further growth of the chain can take place. At even higher concentrations viscosity of the medium increases, which limits the mobility of large monomers and thus favours termination.

Table 4. Conditions and Results of Polymerizations of G2 Macromonomer 23

Entry	monomer conc. (in wt.-%)	M_n ($\times 10^4$)	yield (%)	P_n	P_w	PD
1	33.5	0.42	12	3	3.5	--
2	45.1	0.43	21	3	3.7	--
3	45.1	0.42	20	3	3.6	--
4	49.5	1.70	52	12	20	1.63
5	50.6	3.30	65	22	42	1.82
6	53.2	5.97	88	43	109	2.57
7	53.2	6.50	93	46	110	2.40
8	54.5	4.28	88	30	67	2.20
9	56.6	3.72	86	26	59	2.23
10	56.6	3.90	88	28	64	2.34
11	59.0	3.41	78	24	50	2.07
12	63.6	3.79	83	27	65	2.40

[a)] All polymerizations were performed at 90°C with 3 mol-% of tert-BPB (tert-butylperoxybenzoate) as initiator and toluene as solvent.

[b)] Concentrations in weight percent according to c_m = mon. weight: (mon. weight + solvent weight) × 100%.

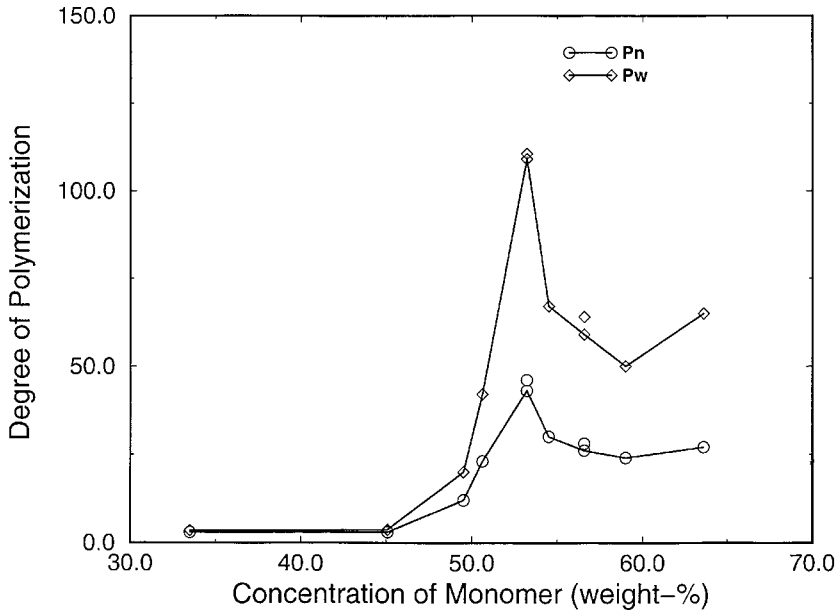

Fig. 12. Dependence of degree of polymerisation on the concentration of monomer **23**.

For a kinetic analysis of the polymerization of G-1 macromonomers, which led the authors to assume that their monomers self-assemble into molecular "reactors" prior to polymerization, see the work of Percec et al.[3,4]

Polymerisation of G3 monomer **24** were carried out in very viscous medium because of the high molar mass. The reaction mixture became solidified after several hours of polymerisation. Owing to the limited amount of monomers, the dependence of degree of polymerisation on concentration of monomer was not obtained.

Table 5. Conditions and Results of Polymerizations of G3 Macromonomer 24

Entry	monomer conc. (in wt.-%)	M_n ($\times 10^4$)	yield (%)	P_n	P_w	PD
1	73	3.3	73	12	18	1.48
2	62	3.7	63	13	20	1.35

For G3 monomer **24**, polymerisations were run two times at different concentration. The conditions and results are listed in Table 5. It can be seen that reasonable molecular weight from G3 monomer **24** was obtained. Considering the high molar mass (above 3,000) of the monomer, the degree of polymerisation is still in the oligomer regime. An increase of the monomer concentration resulted in the increase of conversion, but the DP remained almost unchanged. It should be pointed out that the polydispersity is narrow. The reason for this is not yet clear and needs further investigation.

4.2.4. Deprotection of G2 and G3 polymers 26a and 27a with protected amino functional groups

The deprotections of G2 and G3 polymers **26a** and **27a** were carried out as described for polymer **17a**. The ^{1}H NMR (500 MHz) spectra of polymer **26a** and its deprotected one **26b** are given in Figure 13. As can be seen, the resonances of the protecting groups corresponding to peaks a, b and c disappear. Peak d, which belongs to the protons of protected amine in the polymer, overlaps with the strong absorption of water after deprotection. The strong absorption at $\delta = 3.1$ is assigned to the protons of the terminal methylene protons. The resonances of deprotected polymer are slightly modified.

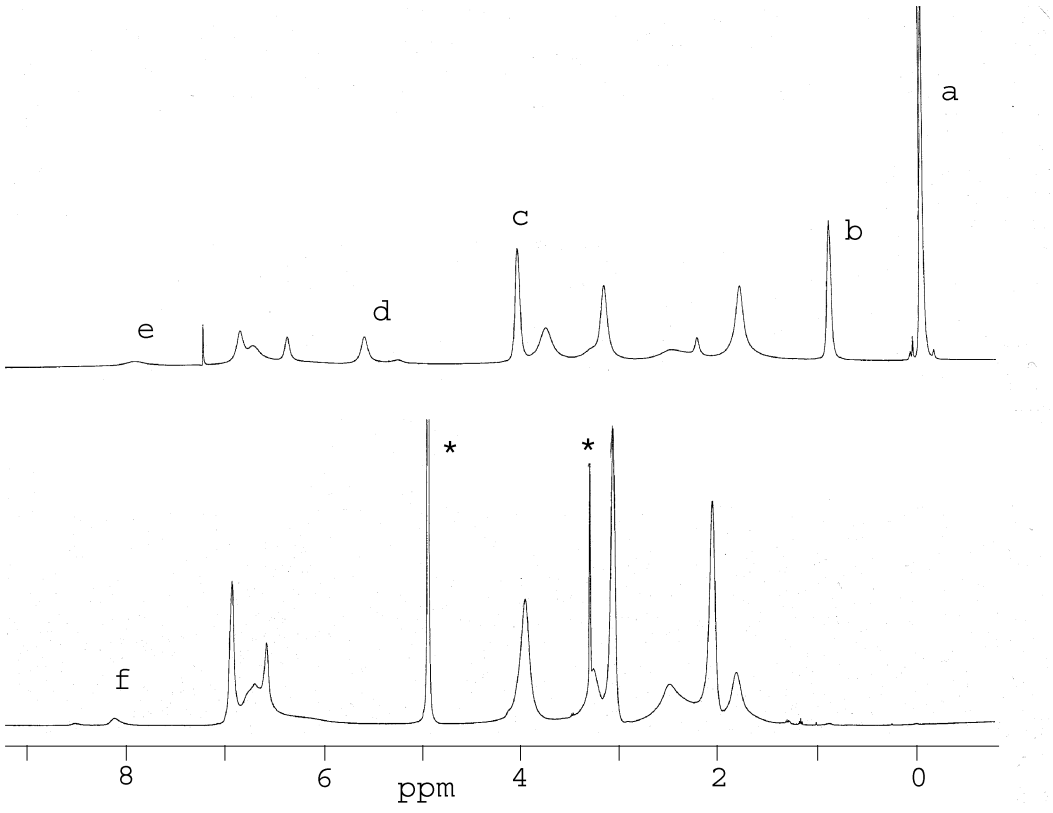

Fig. 13. ^{1}H NMR spectra of polymer **26a** (top) and its deprotected counterpart **26b** (bottom).

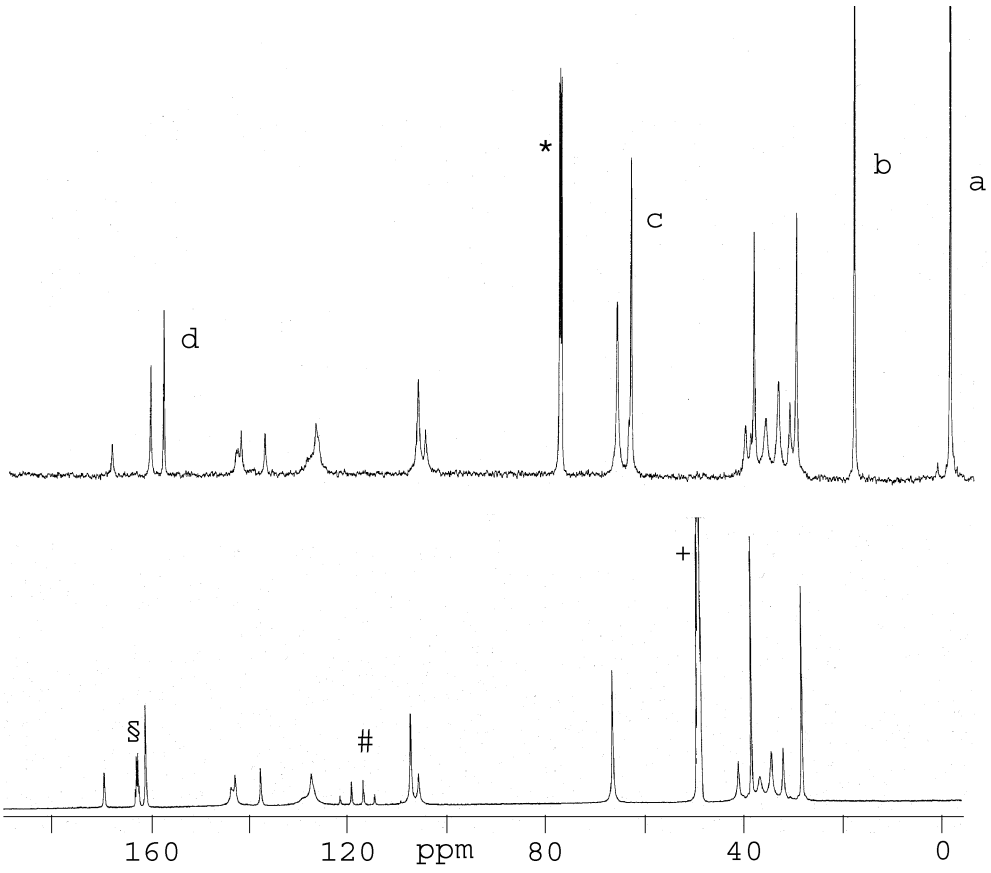

Fig. 14. ^{13}C NMR spectra of polymers **27a** (top) in $CDCl_3$ and its deprotected **27b** (bottom) in CD_3OD. Peaks # and § belong to resonance of CF_3COO^-; peak + is solvent CD_3OD.

compared with those of the starting polymer due to the structural differences and the different solvent used for the measurement. Peaks e and f are assigned to the protons of the inner amide groups. G3 polymer **27a** was deprotected according to the same procedure as **26a**. It can be seen that deprotection is virtually complete from the disappear of peaks a, b and c, which correspond to the Teoc protecting groups (Figure 14).In order to get a good signal to noise ratio, spectrum (bottom) was obtained by using a tube of 1cm in diameter with number of scanning of 19,000 times (overnight). It is obvious that the completeness of deprotection of both the G2 and G3 polymers can be checked by both ^1H and ^{13}C NMR spectra. the deprotection process has no further effect on the polymer structure as should be also concluded from the NMR spectra. This point is very important for the later modification of polymer surface.